Fundamentals of Marine Riser Mechanics

Contents

Preface to the Second Edition

In the new edition, six further chapters, with associated appendices and Excel files, have been added to the original 15 chapters of the first edition. Those original chapters have been left unchanged apart from a small number of minor corrections. The new chapters 16–21 are the fruit of two prolonged dialogues.

The first dialogue was about the effective tension concept and lasted many months. A number of offshore engineers from around the world took part in the discussion about possible objections to the concept. Participants included Andrew Palmer, Joe Fowler, Ivar Fylling, David Garrett, Randy Long, Carl Martin Larsen, Michael Montgomery, Stan Christman, Ron Young, Jack Bayless, and myself.

During those discussions, Jack Bayless played the useful role of imagining every possible argument that could be used to contest the validity of the concept. All except one those arguments were easily answered by referring to the existing literature or the early chapters of this book. The one exception, which had not been previously addressed in the literature, was more difficult to answer. It was finally answered in an article written by myself for *World Oil* in 2012. The argument, and the answer to it, is the principal subject of the new chapter 16. In addition, the effectiveness of buoyancy units, partially or completely embedded in submerged objects, is also discussed in chapter 16, since it is a subject that can also cause confusion.

The second, much longer, dialogue was principally with Stan Christman. It began with a fascinating question about the buckling of a drill pipe inside a cylindrical casing, namely: how, when, and why does initial planar buckling get transformed into helical buckling? That question is only answered in the final chapter 21. Long before the answer was found, the discussion diverged onto the Macondo Accident (Gulf of Mexico, April 2010), with which Stan Christman was intimately concerned as a member of the US Chemical Safety Board investigation team.

Following the Macondo accident, the forensics had shown that the drill pipe had buckled helically inside the riser and that the pipe had deflected laterally inside the subsea BOP to such an extent that it prevented the BOP shear ram from sealing off the well flow. The analytical challenge now became: how closely is it possible to model helical buckling inside a riser associated with flexing of the pipe inside the BOP and downhole, using analytical methods? It took several steps to find the solution.

The first step, which is the subject of chapters 17 and 18, was to find exact expressions for all the forces in a regular helix without using small angle deflection theory.

The second step was to find analytical solutions for helix end sections for a range of end conditions. Continuity at the Annular, at the upper end of the seabed BOP, meant that both the angle and the moment in the drill-pipe would be continuous at that point. Analysis of Helix End Sections with both end angle and end moment is the subject of chapter 19. Such end sections always consist of two parts: a "free-wall section," out of contact with the casing wall, and a "transition section," which is in continuous contact with the casing wall and becomes asymptotic to the regular helix. Analysis of the "free-wall section" is straightforward, but long. The fact that there is an analytical solution at all for the "transition section" can be considered a mathematical miracle. To reach the solution three integrals had to "work," and they most fortunately did so.

The final step, explained in chapter 20, was to link the calculations of the deflection of the different sections of pipe to ensure perfect continuity of angles and moments at their junctions. Those sections include: the regular section and end sections of the helically buckled pipe in the riser, the deflected pipe in the BOP section, and the upper section of the downhole pipe in the well immediately below the BOP, taking into account eventual contact between the pipe and the casing wall. Figure 20–1 shows example elevations of the different sections, obtained using an accompanying Excel file.

I am immensely grateful to Stan Christman for contacting me about this complex and absorbing problem; for the vast number of exchanges we had about it; and for sharing with me his knowledge of BOPs, helical buckling, and the Macondo Accident.

I am also greatly indebted to Jean Falcimaigne for his crucial help in the analysis of the exact forces in a regular helix.

Stan and Jean also helped greatly by rereading and commenting on all chapters and appendixes of the new edition. I am also grateful to the following for their help in commenting on specific chapters: Rob Mitchell, Daniel Averbuch, and Chris Mungall.

Charles Sparks

January 2018

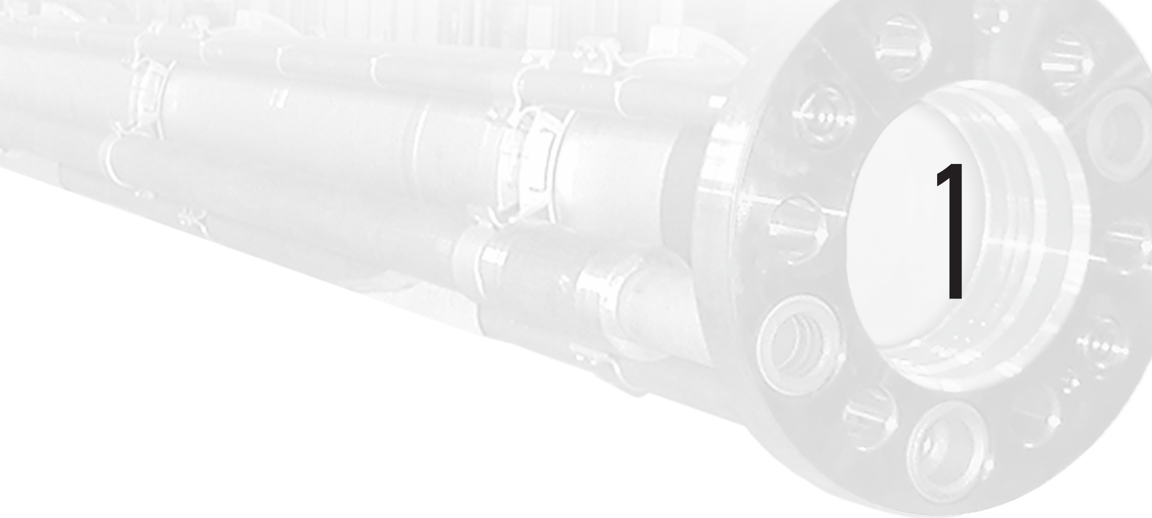

1

INTRODUCTION

This book is principally aimed at explaining the way marine risers behave. It begins with a brief review of the different types of risers that are in use today, with some history and illustrations, as well as references to the types of vessels with which they are associated. Then, an overview of the contents of the following chapters and appendices will be given.

Riser Types

Marine risers date from the 1950s, when they were first used to drill offshore California from barges. An important landmark occurred in 1961, when drilling took place from the dynamically positioned barge CUSS-1. Since those early days, risers have been used for four main purposes:

- Drilling
- Completion/workover
- Production/injection
- Export

Within each group, there is immense variety in the detail, dimensions, and materials, as explained in the following subsections. Drilling risers can be subdivided into low-pressure and high-pressure risers.

Production risers, used from floating platforms, inevitably followed some years after drilling risers. They were first used in the 1970s with an architecture inspired by that of top-tensioned drilling risers. Since then, they have taken many other forms, including bundled risers, flexible risers, top-tensioned risers (TTRs), steel catenary risers (SCRs), and hybrid risers, which are a combination of steel and flexible risers.

can be chosen to give a particular bending effect such as circular bending, or constant bending stresses on the joint outer surface. An Excel file allows the resulting behavior of the joint to be checked numerically.

Chapter 10 looks at the local bending behavior of individual pipes, between guides, in a riser bundle. It is shown that the total moment in the bundle is given correctly by global analysis in which the bundle is simulated as a single structure with the combined characteristics of all the tubes in the bundle (total effective tension, total apparent weight, and total bending stiffness) subject to the sum of lateral loads on all the pipes. However, the distribution of the bending moments between the different pipes depends on several factors, including the load type (apparent weight, hydrodynamic or inertia forces) and the effective tension distribution between the pipes. A further Excel file gives the distribution of moments according to load type, for different data.

Chapter 11 is devoted to TTRs and shows how riser tension and sag evolve with platform offset, particularly when the risers are associated with TLPs or floating platforms. It is shown how riser behavior is influenced by tensioner stiffness, as well as by internal changes to the riser temperature, pressure, and fluid densities. Importantly, even internal changes in a tubing can influence the riser behavior, unless the tubing is equipped with a special, balanced expansion joint designed to avoid such effects.

Chapter 12 looks at the behavior of SCRs. The results obtained in chapter 6 are applied to parts of the catenary. It is deduced that bending stiffness has negligible effect on top tension and on the horizontal component of effective tension (H), for a given total horizontal projection of the total length (suspended part plus seafloor flow line), although the position of the TDP is changed. A simple expression for the change in position of the TDP is given in terms of the bending stiffness and the horizontal force (H). It is also shown that the curvature of a stiff catenary is *greater* than that of a pure catenary over most of its length, which may initially be surprising. Results of numerical simulations are included, which confirm those predictions.

Chapters 13–15 are devoted to riser vibrations. Axial and transverse vibrations are both the result of stress waves that continually ascend and descend a riser. Resonant periods are always equal to twice the time for a stress wave to run between adjacent nodes. Likewise, the time for stress waves to run between adjacent nodes and antinodes are all equal, even when the stress waves are not propagated at constant velocity.

Chapter 13 looks at axial vibration of risers fixed to the seabed at the lower end. Such vibrations are of little consequence in the real world, but

For the other two tubes, *end load* is unhelpful for calculating internal forces because of the changes of diameter and the bends. If instead *end effect* is taken to mean the integral of all pressure-induced axial forces between the section under consideration and the tube end, then it will again give $(p_iA_i - p_eA_e)$ for each tube, where A_i and A_e are the respective internal and external cross-sectional areas at the point under consideration.

In reality, it is impossible to carry out the preceding integral for complicated cases. For example, the ends of the trans-Siberian gas pipeline are separated by thousands of kilometers. In Siberia, the ends are located deep in the earth in a multitude of wells. In Europe, they consist of literally millions of ends in domestic homes! Fortunately, it is not necessary to actually carry out the integral, since the result always gives $(p_iA_i - p_eA_e)$ — that is, the axial force in the internal fluid column less the axial force in the displaced fluid column, at the section concerned.

Nonhorizontal tubes

End loads and end effects can also be helpful in understanding the effect of pressures on perfectly vertical uniform tubes, as explained in appendix B. However, the situation becomes much more confusing for risers, which are neither perfectly vertical nor horizontal. Figure 3–2 shows five near-vertical tubes, all subject to the same effective tension T_e.

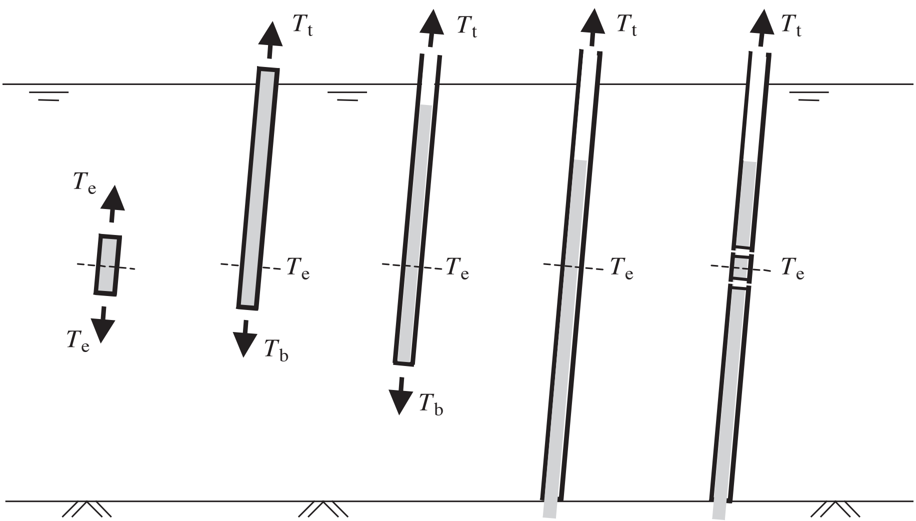

Fig. 3–2. Five near-vertical tubes under pressure

For example, an important parameter in a soil mechanics triaxial test is the difference between the vertical and the horizontal stresses acting on the soil sample, which is also a deviator stress.[3]

Effective Stress and Excess Stress

Effective tension T_e was seen to be the sum of the axial forces in the pipe plus internal fluid column, less the axial force in the displaced fluid column (see the italicized text following equation [2.9]). The reader may therefore be surprised to find effective stress σ_{le}, which is equal to the effective tension divided by the wall section $T_e/(A_e - A_i)$, appearing as a component of the axial stress *in the pipe wall*.[4]

It follows from the equivalence between the effective tension and the excess tension mentioned in chapter 3, preceding equation (3.2). Figure 4–3 shows this equivalence graphically. External pressure has been excluded for clarity. Figure 4–3*a* shows the components of the effective tension, as given in italics following equation (2.9).

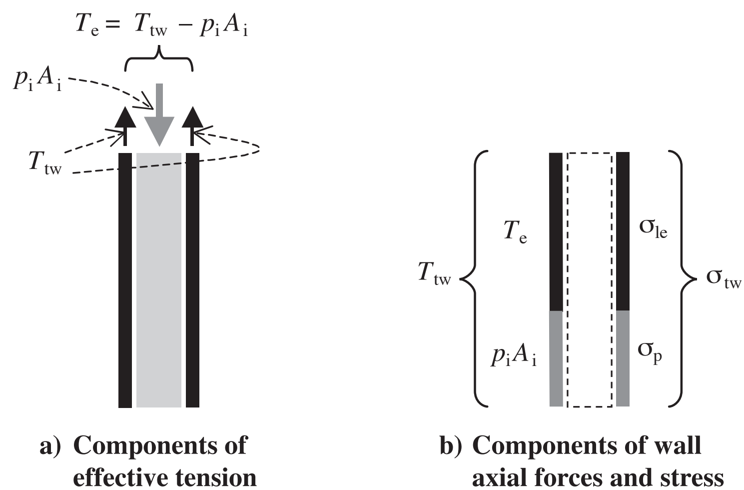

Fig. 4–3. Components of axial forces and stresses in a pipe under internal pressure

The left part of Figure 4–3*b* shows the decomposition of the forces in the pipe wall as given by equation (4.2). The *effective tension* T_e of figure 4–3*a* is plainly always equal to the *excess tension* T_e shown in the left-hand part of figure 4–3*b*. This is no surprise since the equivalence between effective

Riser Tension and Stretch Resulting from Internal Changes

Risers are frequently subject to changes of temperature, pressure, and internal fluids. All these parameter changes will influence the riser tension or axial stretch or both. It is shown below that the relationship between riser top tension T_t and stretch e can always be written in the form

$$T_t = e(k_{riser}) + \{F_w - G_{pt}\} \tag{5.17}$$

where k_{riser} is the riser axial stiffness, F_w is a function of the riser apparent weight, and G_{pt} is a function of riser pressure and temperature.

To find the influence of riser parameters (temperatures, pressures, and internal fluids) on tension and stretch, it is necessary to calculate only the changes ΔF_w and ΔG_{pt} induced by the parameter changes. Then the changes in top tension ΔT_t and stretch Δe are related by

$$\Delta T_t = \Delta e(k_{riser}) + \{\Delta F_w - \Delta G_{pt}\} \tag{5.18}$$

The functions F_w and G_{pt} and, hence, ΔF_w and ΔG_{pt} depend on the riser details. Expressions are derived in the following subsections, first for the case of a uniform riser consisting of a single tube, for which all riser characteristics are assumed to be either constant or to vary linearly over the riser length, and then for a single-tube segmented riser, for which the characteristics are assumed to be constant or linear for each riser segment. Multi-tube risers are examined subsequently. It is not possible to derive general universally applicable expressions for F_w and G_{pt} and, hence, ΔF_w and ΔG_{pt} for multi-tube risers, because of the vast number of different possible combinations. Nevertheless, the procedure to formulate expressions for ΔF_w and ΔG_{pt} for any particular multi-tube riser is explained.

Single-tube uniform risers

For a uniform near-vertical riser tube, with constant linear apparent weight and constant cross-sectional areas A_i and A_e and with characteristics of pressure and temperature varying linearly between the riser extremities, an approach similar to the pipe-upending problem can be used. The axial stretch can be calculated from the initial and final mean values of effective tension, pressure, and temperature at the midpoint of the tube.

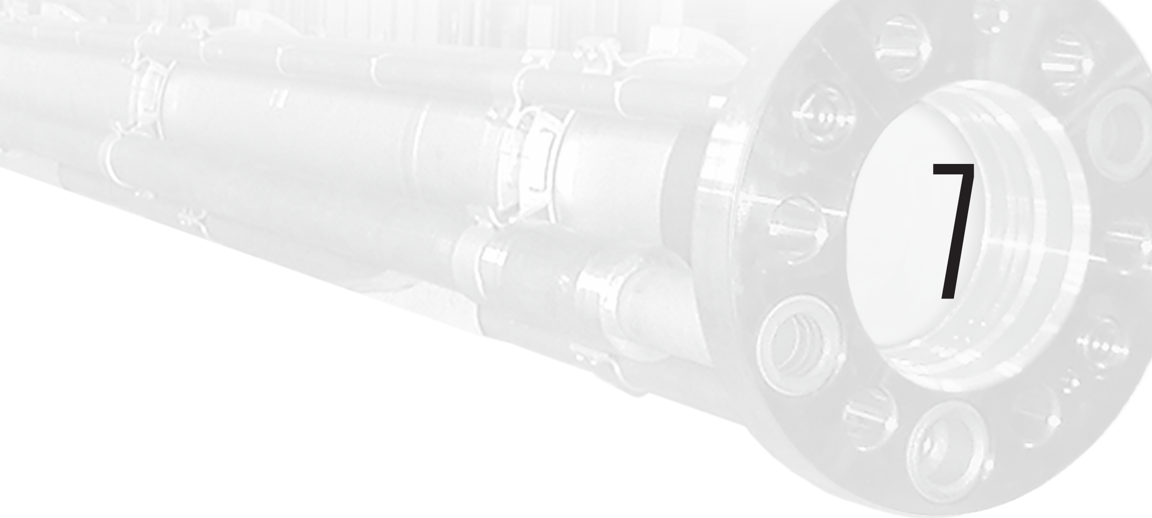

7

STATICS OF NEAR-VERTICAL CABLES

This chapter explores the solution to the riser equation for the case in which tension varies along the length but the bending stiffness is neglected (EI = 0). For simplicity, the corresponding results are referred to as *cable* results.

Once the bending stiffness has been neglected, the differential equation governing the static riser profile (see equation [6.1]) becomes

$$T\frac{d^2y}{dx^2}+w\frac{dy}{dx}+f(x)=0 \tag{7.1}$$

where T is the effective tension and w is the apparent weight. Equation (7.1) can be rewritten as equation (7.2), which can be solved analytically without difficulty:

$$\frac{d}{dx}\left(T\frac{dy}{dx}\right)+f(x)=0 \tag{7.2}$$

Uniform Cable with Current Load

Figure 7–1*a* shows a near-vertical cable with constant apparent weight per unit length, a top-end lateral offset y_t, and a lateral current load function $f(x)$.

At all points along the SJ, the bending radius R_{jx}, the moment M_x and the bending stiffness EI_{jx} are related by $EI_{jx} = M_x R_{jx}$. This, combined with equation (9.11), leads to

$$\frac{EI_{jx}}{EI_{j0}} = \frac{M_x}{M_0}\left(\frac{R_{jx}}{R_{j0}}\right) = \frac{M_x}{M_0}(1+bx) \tag{9.20}$$

Hence, from equation (9.19), the required bending-stiffness function $EI_{j\,x}$ is given by

$$\frac{EI_{jx}}{EI_{j0}} = (1+bx)\left\{1+k_{\text{riser}}x+\left(\frac{k_{j0}}{b}\right)^2\left[(1+bx)\ln(1+bx)-bx\right]\right\} \tag{9.21}$$

If the bending stiffness of the SJ tip is the same as that of the riser and the value of k_{riser} given following equation (9.1) is accepted, then $k_{\text{riser}} = k_{j0}$.

To summarize, the procedure for dimensioning an SJ to obtain constant maximum bending stresses along its length is as follows:

- Determine the forces applied by the riser to the SJ tip—namely, the moment M_0, the associated shear force F_0, and the tension T_0.
- Determine the angle θ_j to be turned through by the SJ.
- Define the required curvature $1/R_{j\,0}$ at the SJ tip and corresponding bending stiffness $EI_{j\,0}$ (since $1/R_{j\,0} = M_0/EI_{j\,0}$). This should take into account the maximum allowable bending stress given by $\sigma_b = E\phi_{e\,0}/2R_{j\,0}$. This bending stress will be constant along the SJ.
- Propose a value for α_j that will apply to the ratios of the radii of curvature $R_{j\,L}/R_{j\,0}$ and to the ratios of the external diameters $\phi_{e\,L}/\phi_{e\,0}$, at the ends of the SJ, as given by equation (9.10).
- Then, the required length of the SJ is given by equation (9.16), and the required bending-stiffness function $EI_{j\,x}$ is given by equation (9.21).

Equation (9.21) defines the required bending-stiffness function to give constant maximum bending stresses along the SJ. The function is valid for any value of the SJ tip moment M_0 (and its associated shear force F_0) and, hence, for any angle through which the SJ is turned. Note, however, that the function is valid only for one value of tension T_0.